



ACCURATE DISCHARGE COEFFICIENT RELATIONSHIP FOR THE CRUMP WEIR

ACHOUR B.^{1}, AMARA L.²*

¹ Professor, Research Laboratory in Subterranean and Surface Hydraulics (LARHYSS),
University of Biskra, Algeria

² Associate Professor, Department of Civil Engineering and Hydraulics, Faculty of
Science and Technology, University of Jijel, Algeria

(*) *bachir.achour@larhyss.net*

Research Article – Available at <http://larhyss.net/ojs/index.php/larhyss/index>

Received May 5, 2022, Received in revised form December 4, 2022, Accepted December 6, 2022

ABSTRACT

Due to its horizontal crest in the transverse direction and its inclined upstream and downstream faces, whose inclination is well defined, the Crump weir can be classified into the category of triangular longitudinal profile weirs, including the Bazin weir. It is an intermediate category between that which includes thin-crested weirs characterized by reduced thickness and that which includes broad-crested weirs that extend over a given length in the streamwise direction.

In practice, the Crump weir is preferably used as a sill for several reasons. The weir reduces the upstream flow velocity by raising the water level, which reduces or even avoids erosion. Additionally, the measurement of the upstream flow depth h , counted above the weir, is carried out with the greatest precision when the device is used as a flow meter.

The Crump weir as a flow measuring structure has not been studied from a theoretical point of view, and only experimental observations have enabled it to be calibrated. The resulting stage-discharge relationship is not only empirical but also incomplete since the effect of influential parameters, such as h/B , where B is the width of the rectangular approach channel, has not been accounted for, which affects the accuracy of the flow rate calculation. Only the effect of the relative elevation of the crest weir $P^* = P/h$ on the flow rate was examined on the basis of observations, where P is the elevation of the crest weir. The dimensionless parameter P^* reflects the influence of the vertical contraction of the flow caused by the weir.

In this study, it is proven that the ratio h/B accounts for 23.5% as an average effect in the calculation of the discharge coefficient C_d and hence of the flow rate Q . The refined model

describing this effect is yielded based on the analysis of observations available in the literature because current theories are unable to produce a mathematical representation of this effect. Unlike h/B , the effect of P^* is derived from a rigorous theory based on the energy equation, judiciously transformed into dimensionless terms, along with rational hydraulic concepts. Therefore, the discharge coefficient relationship resulting from this study is a semiempirical formula that can be written symbolically in the following form

$C_d = \alpha f_1(h/B)f_2(P^*)$. It is inferred that α is a constant whose appropriate value is estimated to be 0.8601, while the symbolic functions f_1 and f_2 are explicitly defined as simple and handy relationships. Compared to recent observations, the previous C_d relationship causes a maximum deviation of only 0.864%, resulting in the same maximum deviation in the flow rate Q computation. Therefore, it can be considered the most accurate and comprehensive C_d relationship ever developed before for the Crump weir working under free overflow conditions. This allows the user to estimate the rate Q sought with great certainty and confidence.

Keywords: Crump weir, stage-discharge relationship, flow measurement, semiempirical approach, discharge coefficient.

INTRODUCTION

The Crump weir belongs to a class between two categories of well-known weirs. The first category includes sharp crested weirs, vertical or inclined, whose classification is based on the shape of the opening, which can be diverse, such as rectangular or triangular notches, which are the most commonly used. They were defined and classified on the basis of both a considerable number of observations of flow profiles and in-depth discharge coefficient investigations (Rao and Muralidhar, 1963; Bos, 1976; Henderson, 1966; Bos, 1989). Their length L in the streamwise direction is reduced to a small thickness, which must meet well-defined design requirements (Achour et al., 2033; SIA, 1936). However, more precisely, sharp-crested weirs are classified as such when h/L varies between 1.5 and 1.9 depending on the particular h/P , according to Rao and Muralidhar (1963), where h is the flow depth above the crest and P is the weir height.

The second category relates to weirs with finite crest length L in the streamwise direction, which are defined quite precisely in the specialist literature (Rao and Muralidhar, 1963; Azimi and Rajaratnam, 2009; Bijankhan et al., 2014). Long-crested weirs, narrow-crested weirs, and broad-crested weirs are listed in this category, according to the range of h/L . Among these weirs, the broad-crested weir is unquestionably the best known and the most used not only as a weir but also as a hydraulic jump control structure and compactness of stilling basins (Achour and Amara, 2022a). It is currently assumed that it shall be said as a "Broad-Crested Weir" any weir freely overflowed by a flow depth h that would vary between $L/10$ and $2L/5$. Consequently, the length L of the weir in the streamwise direction plays a primordial role in this classification. Moreover, it was observed that the discharge coefficient for such a weir is exclusively dependent on h/L , provided that $h/P < 1$.

Additionally, the upstream and downstream faces of these weirs can be vertical, implying a rectangular longitudinal profile, or inclined, which results in a trapezoidal longitudinal profile.

This second category of weirs includes rectangular and triangular cross-section crested weirs, with or without lateral contraction (Rao and Muralidhar, 1963; Bijankhan et al., 2014; Achour and Amara, 2022b; Achour and Amara, 2022c; Achour and Amara, 2022d). However, the question remains whether the triangular broad-crested weir satisfies the aforementioned Rao and Muralidhar requirements or whether other specific hydraulic and/or geometric classification conditions must be found for such a weir.

Between the two aforementioned categories, a third intermediate category could be mentioned, which would include Bazin- and Crump-type weirs (Achour et al., 2033; Bos, 1976; Henderson, 1966; Bos, 1989), which are mainly known for their triangular longitudinal profile. This is the only description, based on the geometry, that is known today of these particular weirs. Their description has not changed since their creation, in such a way as to introduce adapted hydraulic requirements, as was the case for the weirs of the first two categories. These weirs are special because they are endowed with neither a crest length in the streamwise direction nor a reduced thickness. Their crest is reduced to a transverse edge perpendicular to the direction of flow. On either side of this edge, these devices have well-defined inclined walls depending on the type considered. Bazin and Crump's weirs are the only structures that can be listed in this third category and whose cross sections are rectangular. As they are designed, they are not universal ranges since their use as flow measurement devices is restricted to the case of rectangular open channels. However, they have practical advantages thanks to the chosen characteristics of their triangular longitudinal profile, inducing minor solid deposits upstream of the weir as well as the easy evacuation of floating debris. Another significant advantage is that when using these weirs as measurement structures, they give the flow rate Q as a single-valued function of the upstream measured depth h . This aspect of the problem will be developed in detail in the appropriate section of the paper as the primary objective of the study.

The Bazin weir has not been very successful in the practice of measuring flows in open channels. The main reason lies in the fact that it has been calibrated for a weir height $P = 0.50$ m, which is too large to be adapted to the installations of existing factories, including supply channels or waste water discharging channels (Agence Financière du Bassin Loire et Bretagne, 1970). Since then, no study has corrected this drawback through calibration tests to be carried out on much lower crest heights than the original Bazin weir.

The main difference between the Bazin and Crump weirs lies in the values of the slopes of the upstream and downstream faces (Bos, 1976; Henderson, 1966; Bos, 1989; Achour et al., 2003). While Bazin adopted four combinations of upstream and downstream slopes, Crump limited the structure to a single combination, namely, 1:2 upstream and 1:5 downstream, giving the weir a basis length of $L = 7P$. Consequently, the structure can sometimes require much space; for instance, for a weir height $P = 0.30$ m, the weir will

extend over a base length of $L = 2.10$ m, inducing an occupied base surface greater than 3m^2 in the case of a rectangular approach channel that is only 1.50 m wide.

It is worth noting that available stage-discharge relationships that govern the Crump weir are as insufficiently accurate as they are incomplete because they do not take into account all the influential parameters, in particular the h/B ratio, whose average influence is approximately 23.5% according to our conclusive evidence.

Therefore, the study intends to derive the discharge coefficient relationship for the Crump weir and therefore that of the flow rate, as complete as it is accurate, using a semiempirical approach involving both the energy equation and reliable observations available in the literature.

MATERIAL AND METHODS

Description of the device and the resulting flow

Figs. 1 and 2 show the perspective diagram and the longitudinal profile of the Crump weir, respectively. Fig. 2 also exhibits the resulting flow over the weir working under free-flow conditions. The device is intended to measure the flow rate Q conveyed by a rectangular channel of width B , as shown in Fig. 1, where the device was deliberately denoted 'DEVICE'.

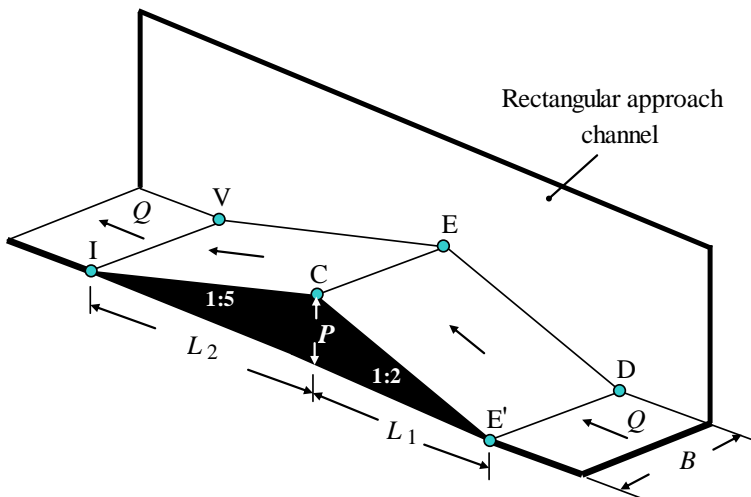


Figure 1: Perspective diagram of the device denoted 'DEVICE' placed in a rectangular approach channel.

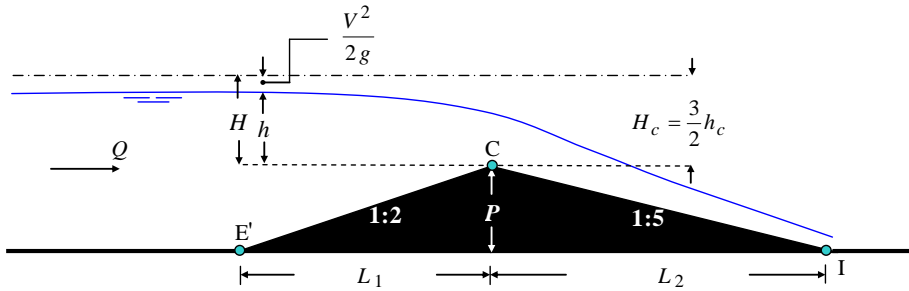


Figure 2: Description of the device and the resulting longitudinal flow profile

As shown in Figs. 1 and 2, the Crump weir is formed by two flat rectangular plates inclined 1:2 upstream and 1:5 downstream; their junction forms, at the top, a horizontal edge in the transverse direction, i.e., perpendicular to the direction of flow, corresponding to the edge CE in Fig. 1.

All models of the Crump weir are designed with a 1:2 sloping front face and a 1:5 sloping back face, forming a triangular longitudinal profile such as the E'CI profile in Fig. 2. Therefore, the lengths L_1 and L_2 (Fig. 2), the sum of which gives the total length of the base of the weir, are such that $L_1 = 2P$ and $L_2 = 5P$, respectively, where P is the crest height.

As seen in Fig. 2, H is defined as the total head counted above the crest of the weir, which is associated with the depth h of the overflowing water nappe. Similarly, V is defined as the mean approach flow velocity, whose quantity $V^2/(2g)$ corresponds to the velocity head. This quantity is generally unwisely neglected in studies relating to the flow measurement, which could lead to significant uncertainties in the calculation of the flow rate sought.

Additionally, as shown in Fig. 2, the flow above the weir crest is assumed to be critical; this is the *sine qua non* condition for the proper functioning of the weir as a flow measurement structure. The control section is considered at point C , where the critical depth is denoted h_c .

The purpose of setting up the weir in the canal is to raise the upstream water level to reach a subcritical regime. Approaching the top of the weir, the flow is accelerated to become supercritical along the upstream face of the weir; the transition from subcritical to supercritical flow is necessarily accompanied by a critical depth that is assumed to manifest at the top of the weir, as indicated previously.

If the geometry of the device is well respected and its installation is properly executed, the flow rate Q is thus determined using only one upstream depth h reading. Thus, the flow rate Q is a single-valued function of the upstream measured depth h , which is well known as a stage. The resulting single-valued function, known as the stage-discharge relationship, can be expressed as $Q = f(h)$, where f is an algebraic function of the stage.

Dimensional analysis and discharge coefficient dependency

The dimensional analysis is interesting insofar as it provides a functional relationship allowing the identification of the influential parameters that affect the sought discharge coefficient. Regarding the Crump weir, one may enumerate eight potentially influential parameters, namely, the discharge Q , the upstream depth h , the crest height P , the rectangular approach channel width B , the acceleration due to gravity g , the density of the flowing liquid ρ , the dynamic viscosity μ of the liquid, and the surface tension σ . These parameters are interrelated by the following functional relationship:

These parameters are interrelated by the following functional relationship:

$$f(Q, \rho, g, h, B, P, \mu, \sigma) = 0 \quad (1)$$

With the help of the Vashy-Buckingham π theorem (Langhaar, 1951), one may derive the following stage-discharge relationship as a function ϕ of dimensionless parameters:

$$Q = g^{1/2} B h^{3/2} \phi \left(\frac{\rho g^{1/2} h^{3/2}}{\mu}, \frac{\rho g h^2}{\sigma}, \frac{h}{B}, \frac{P}{h} \right) \quad (2)$$

Considering the well-known form of the weir equation, one can deduce that function ϕ symbolically expresses the discharge coefficient relationship C_d . Therefore, it is emphasized that the two terms in parentheses of the function ϕ are the Reynolds number Re and the Weber number We . Consequently, the discharge coefficient C_d is functionally written as follows:

$$C_d = \phi \left(Re, We, \frac{h}{B}, \frac{P}{h} \right) \quad (3)$$

Given the turbulent regime of the flow, the Reynolds number Re has no significant effect on C_d . Additionally, the effect of the surface tension expressed by the Weber number We only appears for low flow rates Q and for very narrow channels with a small width B .

Considering the aforementioned considerations, Eq. (3) reduces to:

$$C_d = \lambda \left(\frac{h}{B}, \frac{P}{h} \right) \quad (4)$$

It is thus demonstrated that the discharge coefficient C_d of the considered weir depends on both h/B and P/h . In the field of flow measurement, it is well known that the dimensionless parameter P/h reflects the influence of the vertical contraction of the flow induced by the presence of the weir (Bos, 1976; Henderson, 1966; Bos, 1989; Achour and Amara, 2022c; Achour and Amara, 2022d). The dimensionless parameter h/B is rarely encountered in the stage-discharge relationships that govern flow measurement devices in open channels. This does not mean that its influence is insignificant. Quite the contrary,

as will be seen in the case of the weir under consideration, it has been highlighted that the average effect of h/B on C_d is approximately 23.5%.

In the next sections, through the judicious use of the energy equation, the effect of P/h on the discharge coefficient C_d will be analytically modeled. Unfortunately, the current theories available in the literature are not able to do the same for the effect of h/B ; thus, this will be modeled using observations. Therefore, the function λ will be represented by a semiempirical relationship, which is easy to handle and has unparalleled accuracy.

Theoretical discharge coefficient relationship

Using the energy equation

The Crump weir is formed of rectangular cross-sections, as shown in Fig. 1; then, the critical depth h_c is expressed as follows:

$$h_c = \left(\frac{Q^2}{g B^2} \right)^{1/3} \quad (5)$$

In agreement with Fig. 1 and assuming the kinetic energy correction coefficient is equal to unity, the total head H above the weir crest is written as follows:

$$H = h + \frac{V^2}{2g} \quad (6)$$

Using the continuity equation $V = Q/A$, where A is the water area, Eq (6) becomes the following:

$$H = h + \frac{Q^2}{2g A^2} \quad (7)$$

The water area A can be written as follows (Fig. 2):

$$A = (h + P)B \quad (8)$$

Inserting Eq. (8) into Eq. (7) yields the following:

$$H = h + \frac{Q^2}{2g B^2 (h + P)^2} \quad (9)$$

Additionally, neglecting any kind of head loss, one may assume that the total head H is equal to the total critical head H_c , as indicated in Fig. 2. Thus, one may write the following equality:

$$H = h + \frac{Q^2}{2gB^2(h+P)^2} = H_c = \frac{3}{2}h_c \quad (10)$$

It is worth noting that the constant 3/2 on the right-hand side of Eq. (10) is an ideal value; however, the reality is quite different, as has been shown by a very thorough previous study (Khafagi, 1942). The actual observed constant is less than 3/2 depending on the value of the angle of inclination formed by the free surface of the falling water nappe with respect to the horizontal.

For instance, if the free-surface inclination is approximately 19°, then, using simple theoretical considerations, one may derive that the constant will take the value 1.48 instead of the value 1.50 consistently being admitted regardless of the approach flow conditions. The experimental verification of Khafagi (1942) showed clear evidence of this discrepancy.

Additionally, since the finding of this important result in the 1940s, no study has been carried out to examine the influence of this discrepancy on major hydraulic problems, including those related to the field of flow measurement, which is often based on the principle of critical flow.

Considering Eq. (10), the following is extracted:

$$h + \frac{Q^2}{2gB^2(h+P)^2} = \frac{3}{2}h_c \quad (11)$$

Eliminating the discharge Q between Eqs. (5) and (11) results in the following:

$$h + \frac{h_c^3}{2(h+P)^2} = \frac{3}{2}h_c \quad (12)$$

Let us define the following dimensionless parameters:

$$P^* = \frac{P}{h} \quad (13)$$

$$h^* = \frac{h}{h_c} \quad (14)$$

Thus, Eq. (12) can be rewritten in the following dimensionless form:

$$h^* + \frac{1}{2h^{*2}(1+P^*)^2} = \frac{3}{2} \quad (15)$$

After some manipulations and arrangements, Eq. (15) is reduced to the following cubic equation in h^* , including a quadratic term:

$$h^*{}^3 - \frac{3}{2}h^*{}^2 + \frac{1}{2}(1 + P^*)^{-2} \quad (16)$$

What emerges from Eq. (16) is that the relative depth h^* depends solely on the relative crest height P^* .

Eq. (16) has three real roots, of which only one satisfies the physical condition $h^* > 1$ since $h > h_c$. Using the solving method described by Spiegel (1974), the real root of Eq. (16), which satisfies the physical meaning of the problem, regardless of the P^* value, is the following:

$$h^* = \cos \left[\frac{1}{3} \cos^{-1}(\psi) \right] + \frac{1}{2} \quad (17)$$

where the dimensionless parameter ψ is expressed as follows:

$$\psi = 1 - 2(1 + P^*)^{-2} \quad (18)$$

Additionally, eliminating the critical depth h_c between Eqs. (5) and (14) results in the following discharge Q relationship:

$$Q = \frac{\sqrt{2}}{2} \sqrt{2g} h^{*-3/2} B h^{3/2} \quad (19)$$

Given that the discharge coefficient of any device can be defined as the ratio of the actual discharge to the theoretical discharge, Eq. (19) can be written in the following well-known form of the weirs stage-discharge relationship:

$$Q = C_d \sqrt{2g} B h^{3/2} \quad (20)$$

where C_d is the discharge coefficient of the weir under consideration. Comparing Eqs. (19) with (20) yields the following discharge coefficient relationship:

$$C_d = \frac{\sqrt{2}}{2} h^{*-3/2} \quad (21)$$

Combining Eqs. (17) and (21) results in the following:

$$C_d = \frac{\sqrt{2}}{2} \left\{ \cos \left[\frac{1}{3} \cos^{-1}(\psi) \right] + \frac{1}{2} \right\}^{-3/2} \quad (22)$$

Eq. (22) expresses the theoretical discharge coefficient of the Crump weir for which the known parameter in practice is P^* , which allows computing the parameter ψ according to Eq. (18). Additionally, Eq. (22) implicitly reflects the effect on the discharge coefficient C_d of the vertical contraction that the flow undergoes due to the weir.

It is planned that the reliability and validity of Eq. (22) will possibly be corroborated using the observations available in the literature or corrected if necessary.

Using the kinetic factor

The total H expressed by Eq. (6) can be written in the following form:

$$H = h + \delta h \tag{23}$$

where δ is a dimensionless parameter representing the fraction of the head in relation to the kinetic energy. In other words, one may write δ as follows: $\delta = V^2 / (2 g h)$. Thus, to better understand the physical significance of the kinetic factor δ , let us write it as $\delta = (V / \sqrt{2 g h})^2$; hence, one may observe that it corresponds to the ratio of the actual mean flow velocity to the ideal flow velocity given by Torricelli. Moreover, when the conditions of the critical flow are satisfied in the approach channel, corresponding to the ratio $V / \sqrt{g h} = 1$, $P^* = 0$, and $h^* = 1$, then it can be derived that $\delta = 1/2$, which is the greatest value that the kinetic factor δ can reach.

Eq. (23) can be rewritten in the following form:

$$H = h (1 + \delta) \tag{24}$$

Additionally, writing Eq. (9) in the form of Eq. (24) results in:

$$\delta = \frac{Q^2}{2 g B^2 h (h + P)^2} \tag{25}$$

Furthermore, when combining Eqs. (10) and (24), one may derive the following:

$$H = \frac{3}{2} h_c = (1 + \delta) h \tag{26}$$

When eliminating the critical depth h_c between Eqs. (5) and (26), this results in the following:

$$Q^2 = \left(\frac{2}{3}\right)^3 g B^2 (1 + \delta)^3 h^3 \tag{27}$$

Furthermore, eliminating the discharge Q between Eqs. (25) and (27) yields the following:

$$\delta = \frac{\left(\frac{2}{3}\right)^3 g B^2 (1 + \delta)^3 h^3}{2 g B^2 h (h + P)^2} \tag{28}$$

Introducing the dimensionless parameter P^* defined by Eq. (13) and simplifying, Eq. (28) reduces to the following:

$$\delta = \frac{1}{2} \left(\frac{2}{3} \right)^3 \frac{(1 + \delta)^3}{(1 + P^*)^2} \quad (29)$$

Let us assume ξ governed by the following relationship:

$$\xi = \frac{27}{4} (1 + P^*)^2 \quad (30)$$

Thus, Eq. (29) is reduced to the following:

$$(1 + \delta)^3 - \xi \delta = 0 \quad (31)$$

Eq (27) is a cubic equation with a quadratic term, expressed as:

$$\delta^3 + 3\delta^2 - (\xi - 3)\delta + 1 = 0 \quad (32)$$

Eq. (28) admits three real solutions, only one of which satisfies the physical condition $\delta < 1$.

Using the third-degree solution method described by Spiegel [16], the solution sought is as follows:

$$\delta = 3\varphi^{-1} \cos \left[\frac{1}{3} \cos^{-1}(-\varphi) + \frac{4\pi}{3} \right] - 1 \quad (33)$$

where

$$\varphi = (1 + P^*)^{-1} \quad (34)$$

However, when rewriting Eq. (27) in the form of Eq. (20) results in the following C_d relationship:

$$C_d = \frac{1}{\sqrt{2}} \left(\frac{2}{3} \right)^{3/2} (1 + \delta)^{3/2} \quad (35)$$

Inserting Eq. (33) into Eq. (35), the final relationship governing the discharge coefficient C_d is as follows:

$$C_d = 2 \left\{ \varphi^{-1} \cos \left[\frac{1}{3} \cos^{-1}(-\varphi) + \frac{4\pi}{3} \right] \right\}^{3/2} \quad (36)$$

Although derived from two different methods, Eqs. (22) and (36), however, give the same result.

The kinetic factor δ is a parameter that studies on flow measurement tend to neglect, which could lead to unsuitable results. According to Eq. (35), if the approach flow velocity were to be neglected, i.e., $\delta \rightarrow 0$, regardless of the given value of P^* , then the discharge coefficient of the Crump weir would be considered constant, such as:

$$C_d = \frac{1}{\sqrt{2}} \left(\frac{2}{3} \right)^{3/2} = 0.3849 \quad (37)$$

However, for the sake of rigor, the kinetic factor δ is equal to 0 only for $P^* \rightarrow \infty$, according to Eq. (34) for $\varphi \rightarrow 0$. Thus, under these conditions, Eq (36) gives $C_d \rightarrow 0.3849$ for the Crump weir, which seems to be in disagreement with what is observed on the broad-crested weir, for which $C_d = 0.3849$ for $P^* \rightarrow 0$ (Bolshakov, 1984). According to Eq. (36) along with Eq. (34), the discharge coefficient C_d of the Crump weir is 0.7071 for $P^* \rightarrow 0$. In reality, there is no disagreement between the observations made on the discharge coefficients of the two devices for $P^* \rightarrow 0$. Under this limit condition, the discharge Q through the broad-crested weir can be written as $Q = 0.3849 \sqrt{2g} B H^{3/2}$, where H is the total head over the weir, including the velocity head. Additionally, the critical flow condition prevailing on the broad-crested weir allows us to write that $H = (3/2) h_c$.

Thus, the discharge Q can be rewritten as $Q = 0.3849 (2/3)^{3/2} \sqrt{2g} B h^{3/2}$, which has the same form as Eq. (20), meaning that $C_d = 0.3849 (3/2)^{3/2}$. Therefore, one may finally derive that $C_d = 0.7071$ corresponding to the same value of the Crump weir discharge coefficient obtained for the same limit condition $P^* \rightarrow 0$.

In any case, it is not recommended to neglect the kinetic factor δ , as it does not reflect reality. As seen in the last column of Table 1, this simplifying assumption would generate significant deviations in the calculation of the discharge coefficient C_d , depending on the P^* value.

Additionally, Table 1 shows that the kinetic factor δ decreases with the increase in the relative crest height P^* of the weir. Furthermore, as previously indicated, the kinetic factor δ is less than $1/2$ for $P^* > 0$ or equal to $1/2$ for $P^* = 0$ or $h^* = 1$ according to Eq. (17) along with Eq. (18), i.e., at the critical flow condition in the approach channel.

What Table 1 reveals most importantly is that the kinetic factor δ ought not to be neglected, regardless of the value of P^* involved, because the deviations that could be caused in the calculation of C_d are significant. The deviations reported in the last column of Table 1 also correspond to those caused in the calculation of the flow rate Q according to Eq. (20). Such deviations are not often tolerated in many practical situations, especially those that require high accuracy in the flow rate calculation.

Table 1: Values of the kinetic factor δ for some values of the relative crest height P^* of the weir according to Eq. (29)

P^*	δ Eq. (29)	$(1 + \delta)^{3/2}$	$\Delta C_d / C_d$ (%)
0	0.5	1.83711731	83.71
0.2	0.161003	1.25097898	25.98
0.4	0.100833	1.15500047	15.50
0.6	0.071115	1.1085471	10.85
0.8	0.053456	1.08124622	8.12
1	0.041889	1.06348698	6.35
1.2	0.033821	1.05115806	5.11
1.4	0.027936	1.04219531	4.22
1.6	0.023497	1.03545174	3.54
1.8	0.020056	1.03023434	3.02
2	0.017332	1.02611033	2.61
2.2	0.015134	1.02278667	2.28
2.4	0.013335	1.02006904	2.00
2.6	0.011842	1.01781548	1.78
2.8	0.010589	1.01592547	1.59
3	0.009526	1.01432298	1.43

Incident Froude number

The Froude number is a dimensionless parameter describing flow regimes in open channels. It is defined as the ratio of inertia forces to gravitational forces (Bos, 1976; Henderson, 1966, Cow, 1959), meaning that it is a parameter measuring the ratio of the inertia force on an element of fluid to the weight of the fluid element. The Froude number is relevant in open-channel flow problems where the weight, related to gravitational force, of the flowing water is an important force. This is the current case that concerns the upstream flow in the approach channel, which is characterized by a predominance of gravitational forces compared to inertia forces, meaning that the flow is subcritical, resulting in an incident Froude number less than unity. In a subcritical state, the flow is controlled from downstream, meaning that any disturbance that occurs at a downstream point is transmitted upstream. In the case that concerns the present study, the disturbance is reflected by the presence of the weir; therefore, a close relationship between the characteristics of the weir and the incident Froude number is expected.

Additionally, in the field of flow measurement in open channels, the user must ensure an upper limit value of the incident Froude number to prevent waves from disturbing accurate upstream depth readings. There are no in-depth studies on this subject, and only experimentation recommends that the incident Froude number be less than 0.50 (Agence Financière du Bassin Loire et Bretagne, 1970).

Let us define the incident Froude number of the upstream flow by F_o , corresponding to the depth $(h + P)$ in Fig. 1. Thus, one may write the following:

$$F_o = \frac{V}{\sqrt{g(h + P)}} \tag{38}$$

Using the continuity equation $V = Q/A$, where the wetted area A is $A = B(h + P)$, Eq (38) becomes the following:

$$F_o = \frac{Q}{\sqrt{g} B(h + P)^{3/2}} \tag{39}$$

After some manipulations, Eq. (39) can be rewritten as follows:

$$F_o = \frac{Q}{\sqrt{g} B h^{3/2} (1 + P^*)^{3/2}} \tag{40}$$

Combining Eqs. (5), (14), and (40) yields the following:

$$F_o = [h^* (1 + P^*)]^{-3/2} \tag{41}$$

Inserting Eq. (17) into Eq. (41) results in the following:

$$F_o = \left\{ \left(\cos \left[\frac{1}{3} \cos^{-1}(\psi) \right] + \frac{1}{2} \right) (1 + P^*) \right\}^{-3/2} \tag{42}$$

As the dimensionless parameter ψ depends only on the relative height P^* of the weir in accordance with Eq. (18), Eq. (42) indicates that the incident Froude number F_o depends solely on P^* , meaning that it is fully controlled by the relative height of the weir, as expected.

The variation in the incident Froude number F_o as a function of P^* is represented in Fig. 3 according to Eq. (42).

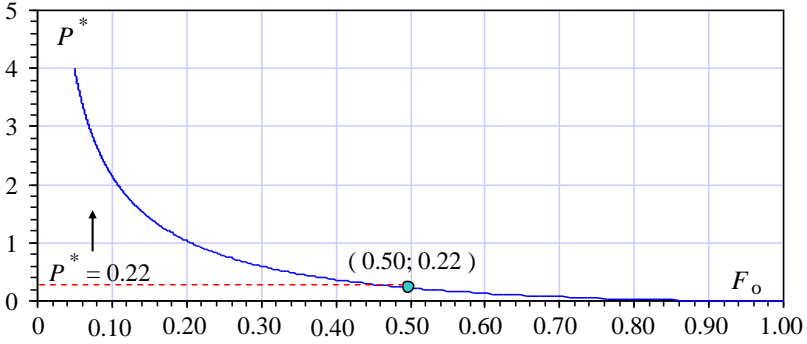


Figure 3: Variation in the incident Froude number F_o against P^* according to Eq.(42)

As seen, the greater the relative height P^* increases, the greater the incident Froude number F_o decreases. For $P^* \rightarrow 0$, the incident Froude number is $F_o \rightarrow 1$, meaning that the upstream flow depth tends to become critical. In addition, if the recommendations reported in the literature were to be respected, advising F_o less than 0.50, then the relative height P^* of the weir to be considered should be greater than 0.22, as indicated in Fig. 3.

On the other hand, Eq. (38) can be rewritten in the following form:

$$F_o = \frac{V}{\sqrt{g h (1 + P^*)}^{1/2}} \quad (43)$$

Additionally, it was previously deduced that the kinetic factor δ is such that $\delta = (V / \sqrt{2 g h})^2$, which allows us to transform equation (43) as follows:

$$F_o = \sqrt{\frac{2 \delta}{1 + P^*}} \quad (44)$$

That is,

$$\delta = \frac{1}{2} (1 + P^*) F_o^2 \quad (45)$$

This relationship relates the kinetic factor δ to the incident Froude number F_o . When the upstream flow tends to be critical, corresponding to $P^* \rightarrow 0$ and $F_o \rightarrow 1$, Eq. (45) gives $\delta \rightarrow 1/2$, which is the greatest value that the kinetic factor δ can reach, as stated in one of the previous sections, using, however, a different approach.

If the incident Froude number F_o was to be limited to 0.50, corresponding to the lower limit value $P^* = 0.22$, then Eq. (45) shows that the kinetic factor δ should not exceed the upper limit value of 0.1525.

RESULTS

This section aims to validate or possibly correct the relationships derived from the previously suggested theoretical approach. The observations available in the literature that are the aptest to be exploited are the twenty-three experimental values of the pair (Q ; h) provided by Zuikov (2017). These were collected on a Crump weir with a weir height $P = 0.07$ m and tested in a rectangular approach channel with a width $B = 0.311$ m. The flow rate Q was varied in the range [1.45 l/s; 31.81 l/s], corresponding to the following range of variation [1.71 cm; 12.30 cm] of the resulting flow depth h . Table 2 gathers the experimental data of Zuikov (2017) used during the present study.

With the help of the experimental values of the depth h given in Table 2, as well as the weir height set at $P = 0.07$ m, the experimental dimensionless parameter P^* was calculated by Eq. (13), allowing us to deduce the corresponding values of the parameter ψ using Eq. (18). Thus, introducing the computed values of ψ into Eq. (17) resulted in the theoretical values of h^*_{Th} , where the subscript “Th” denotes “Theoretical”. On the other hand, the experimental values of the discharge Q given in Table 2 along with the width $B = 0.331$ m of the approach channel were used to calculate the resulting critical depth h_c values in accordance with Eq. (5). Thus, inserting the computed values of h_c as well as the experimental values of the depth h given by Table 2 into Eq. (14) yields the values of h^*_{Exp} , where the subscript “Exp” denotes “Experimental”. Finally, h^*_{Exp} and h^*_{Th} are plotted in Fig. 4 against ψ .

Table 2: Zuikov’s observations (2017) collected on a Crump weir 0.07 m in height

Run	Q (m ³ .s ⁻¹)	h (m)
1	0.00145278	0.0171
2	0.00280833	0.0263
3	0.00417778	0.0341
4	0.00554167	0.0407
5	0.00699444	0.0478
6	0.00829722	0.0528
7	0.00972222	0.0586
8	0.01110556	0.0641
9	0.01248611	0.0688
10	0.01393611	0.0737
11	0.01523889	0.0781
12	0.0167	0.0825
13	0.01804722	0.0863
14	0.01942222	0.0908
15	0.02088056	0.0948
16	0.02226944	0.0987
17	0.02365278	0.1026
18	0.02504167	0.106

19	0.02641944	0.1093
20	0.02786111	0.113
21	0.02923889	0.1165
22	0.03054722	0.1195
23	0.03181667	0.123

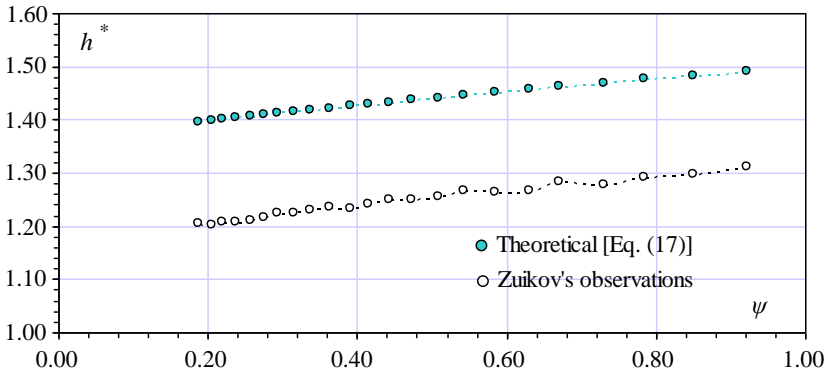


Figure 4: Variation in the experimental and theoretical relative depths h^* as a function of ψ

First, Fig. 4 is able to provide reliable indications regarding the quality of Zuikov's observations (2017). Thus, it can be observed that some measurement points deviate somewhat from the general trend of the curve, which means that they are marred by an error, probably due to the reading of the depth h , the flow rate Q , or even both. However, Fig. 4 indicates that, overall, Zuikov's observations [19] are of sufficiently high quality to enable reliable analysis.

The theoretical values of h^* , computed using Eq. (17) along with Eq. (18), are greater than those derived from Zuikov's observations (2017). The striking observation that one must be drawn from Fig. 4 is related to the resulting curves whose variation follow an almost similar evolution, as if, at first sight, they are just shifted by a certain constant. The calculation somewhat confirms this observation since deviations between theoretical values of h^* according to Eq. (17) and the experimental values according to Zuikov's observations vary in the following restricted range [12%; 14%]. Moreover, the ratio h^*_{Exp}/h^*_{Th} varies between 0.860 and 0.879.

This almost constant shift between the theoretical and experimental curves is also observed in the variation of discharge coefficients C_d , as shown in Fig. 5. The experimental discharge coefficient was calculated according to Eq. (20) for $Q = Q_{Exp}$ and $h = h_{Exp}$, while the theoretical discharge coefficient was derived from Eq. (22) along with Eq. (18) for $P^* = P^*_{Exp}$.

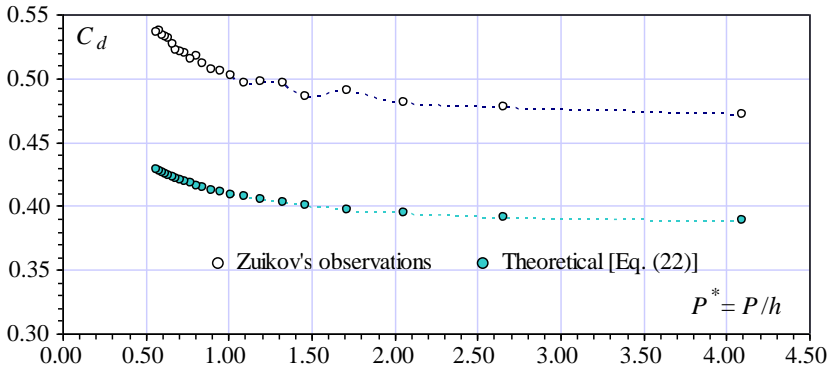


Figure 5: Variation in the experimental and theoretical discharge coefficients C_d as a function of the relative weir height P^*

An in-depth study led us to conclude with certainty that the deviations observed in the experimental and theoretical values of h^* , and hence those of C_d , are largely due to the unsuspected effect of the relative depth h/B that previous studies have not accounted for. Calculations revealed that the average effect of h/B on the flow coefficient C_d could be estimated at 23.5%.

Two formal suggestions can be made to the user. The first one, if preferred, consists of a simplified approach to derive a stage-discharge relationship for the Crump weir that gives a fast result along with acceptable accuracy. For this, it is recommended to consider the effect of h/B on h^* , and hence on the flow rate Q , as an average causal effect that occurs through a constant. This corresponds to the average value of all the h^*_{Exp}/h^*_{Th} ratios involved, resulting in a value of 0.8687. Thus, one may write the following:

$$\frac{h^*_{Exp}}{h^*_{Th}} \approx 0.8687 \tag{46}$$

Combining Eqs. (21) and (46) results in the following final discharge coefficient relationship:

$$C_d = 0.8733 h^{*-3/2} \tag{47}$$

Inserting Eq. (17) governing h^* into Eq. (47) yields the following:

$$C_d = 0.8733 \left\{ \cos \left[\frac{1}{3} \cos^{-1}(\psi) \right] + \frac{1}{2} \right\}^{-3/2} \tag{48}$$

Let us recall that the parameter ψ is given by Eq. (18) for the known value of P^* . It is worth noting that Eq. (48) is valid in the following experimental ranges:

$$0.569 \leq P^* \leq 4.093, 0.055 \leq h/B \leq 0.395$$

The maximal deviation caused by Eq. (48) is 1.708%, which also corresponds to the maximal deviation caused in the flow rate Q computation according to Eq. (20). This maximum deviation is much lower than the maximal deviation value of 4.909% caused by the recent empirically derived stage-discharge relationship available in the literature (Zuikov, 2017), as reported in Table 3.

The second formal suggestion is the most rigorous, inducing much more accurate results, although it requires additional computation. It no longer considers an average causal effect of h/B on h^* , but it relies on a more elaborated and refined model of correction of h^* as a function of h/B , such as writing the following:

$$h^*_{Exp} = 0.8776 \left[1 - 1.936 \left(\frac{h}{B} \right)^{1.337} \right]^{0.0252} h^*_{Th} \quad (49)$$

Thus, when considering Eqs. (17) and (49), the relative depth h^* is then expressed as follows:

$$h^* = 0.8776 \left[1 - 1.936 \left(\frac{h}{B} \right)^{1.337} \right]^{0.0252} \left\{ \cos \left[\frac{1}{3} \cos^{-1}(\psi) \right] + \frac{1}{2} \right\} \quad (50)$$

Eq. (50) causes a maximum deviation of 0.573% in the h^* calculation, which corresponds to a maximum deviation in C_d computation of 0.864% according to Eq. (21). This finding was corroborated by an in-depth analysis of the observations provided by the literature (Zuikov, 2017). With the help of Eq. (50), Eq. (41) gives the appropriate value of the incident Froude number F_o for the given value of the relative weir height P^* .

It is worth noting that the maximal deviation in the h^* computation, which was 14% as previously mentioned, dropped to only 0.573%, which reveals the importance of the effect of h/B on h^* and hence on the discharge coefficient C_d . It must be noted that the h^* correction model expressed by Eq. (50) is also valid in the aforementioned ranges of P^* and h/B . Therefore, when considering both Eqs. (21) and (50), the discharge coefficient C_d of the Crump weir is written in the following final form:

$$C_d = 0.8601 \left[1 - 1.936 \left(\frac{h}{B} \right)^{1.337} \right]^{-0.0377} \left\{ \cos \left[\frac{1}{3} \cos^{-1}(\psi) \right] + \frac{1}{2} \right\}^{-3/2} \quad (51)$$

It is useful to remember that the parameter ψ is given by Eq. (18) for the known value of P^* . Eq. (51) is a semiempirical relationship because the effect of h/B on the discharge

coefficient C_d has been supported and modeled using experimental data available in the literature (Zuikov, 2017).

As already indicated, the maximum relative error caused by Eq. (51) on the calculation of C_d is 0.864%, which also corresponds to the maximum deviation caused in the calculation of the flow rate Q according to Eq. (20).

Additionally, it should be noted that both terms "Precision" and "Accuracy" are often used confusingly in many studies since the term "Deviation" is not clearly defined or interpreted incorrectly. Deviation or relative error (RE), considered herein, does not refer to the precision of a measurement, which is defined as the ratio of the absolute error of a measurement to the measurement being taken (Agresti, 1990; Vogt and Johnson, 2015; Abramowitz and Stegun, 1972). The RE is used herein to describe accuracy, specifically how accurate the semiempirical Eq. (51) is, which gives expected or accepted C_d values when compared to C_d experimental values estimated using Eq. (20) for $Q = Q_{Exp}$ and $h = h_{Exp}$. Thus, the appropriate formula used herein to compute RE is the following:

$$RE (\%) = \left| \frac{C_{d,Experimental} - C_{d,Expected}}{C_{d,Expected}} \right| \times 100 \tag{52}$$

where the vertical bars denote absolute values.

Fig. 6 shows the distribution of deviations induced by Eq. (47) in the calculation of the discharge coefficient C_d plotted against the relative discharge $Q/[gB^5]^{1/2}$. As seen, 100% of the deviations are less than 0.865%, which allows us to state, with complete assurance, that the derived semiempirical Eq. (47) governing the discharge coefficient of the Crump weir is highly accurate. Moreover, Eq. (51) is incomparably more accurate than the formulas available in the literature (Zuikov, 2017; Filippov and Brakeni, 2007; RF State Standard MI 2406–97, 1997). This is confirmed by Table 3 reporting deviations caused by the authors' Eq. (51) and those induced by the last developed formula disclosed in the literature.

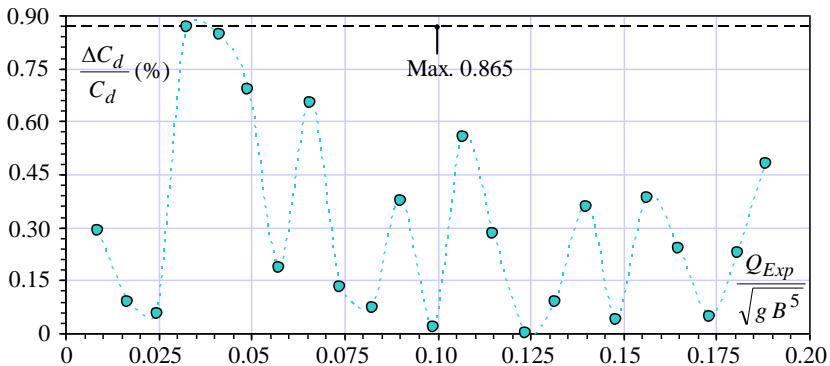


Figure 6: Deviations in the discharge coefficient C_d computation caused by Eq. (51)

Table 3: Comparison between deviations in the C_d computation of the Crump weir induced by Eq. (51) and the Zuikov relationship (2017)

Reference	Deviation $\Delta C_d / C_d$ (%)			Validity ranges
	Minimum	Maximum	Average	
Eq. (51)	0.00061	0.864	0.302	$0.569 \leq P^* \leq 4.093$ $0.055 \leq h/B \leq 0.395$
Zuikov (2017)	0.0445	4.909	1.429	

CONCLUSION

The Crump weir, which is of practical use as a measuring structure, has been the subject of both theoretical and empirical investigations. The main objective was to determine the discharge coefficient relationship of such a device and hence the resulting stage-discharge equation.

Dimensional analysis revealed that the P/h and h/B ratios are the only influential parameters, where h is the upstream depth of the flow above the weir crest, B is the width of the approach rectangular channel, and P is the height of the weir.

The influence of the first parameter on the discharge coefficient C_d of the device was modeled by a rigorous analytical approach based on the energy equation presented in dimensionless terms. Particular care was taken to include the effect of the approach flow velocity. However, the advocated theoretical approach was not able to model the effect of the second influential parameter, i.e., h/B . For this, it was called upon observations available in the literature to provide an accurate model describing the effect of h/B .

Thus, the discharge coefficient C_d relationship governing the Crump weir has been built, which causes a maximum deviation of only 0.864%, allowing us to henceforth rank the Crump weir among the most accurate flow measurement structures. The resulting C_d relationship, whose accuracy is probably unrivalled with regard to the results reported in the literature, was presented as a product of a constant and two functions f_1 and f_2 dependent on h/B and P^* , respectively.

If the experimental data concerning the Crump weir were available for various values of the weir height P , then it would have been interesting to check whether the model describing the effect of the second influential parameter would have been more precise by considering the quantity $(h + P)/B$ instead of h/B . This issue could be considered in future studies.

Declaration of competing interest

The authors declare that they have no known competing financial interests or personal relationships that could have appeared to influence the work reported in this paper.

REFERENCES

- ABRAMOWITZ M., I.A. STEGUN I.A. (1972). Handbook of Mathematical Functions with Formula, graphs, and Mathematical Tables, 9th printing, 1972, p.14, New York: Dover.
- ACHOUR B., AMARA L. (2022a). Compactness of Hydraulic Jump Rectangular Stilling Basins Using a Broad-Crested Sill, Larhyss Journal, No 51, pp. 31-41.
- ACHOUR B., AMARA L. (2022b). Theoretical and experimental investigation of a lateral broad-crested contraction as a flow measurement device, Flow Measurement and Instrumentation, Vol. 86, Paper 102175.
- ACHOUR B., AMARA L. (2022c). Flow measurement using a triangular broad crested weir theory and experimental validation, Flow Measurement and Instrumentation, Vol. 83, Paper 102088.
- ACHOUR B., AMARA L. (2022d). Rectangular broad-crested flow meter with lateral contraction - Theory and experiment, Larhyss Journal, No 49, pp. 85-122.
- ACHOUR B., BOUZIANE M.T., NEBBAR K. (2003). Broad-crested triangular flowmeter in rectangular channel, Larhyss Journal, No 2, pp. 7-43 (In French).
- AFBLB, Agence Financière du Bassin Loire et Bretagne (1970). Book of special requirements for the production and approval of devices for measuring the flow of effluents, (In French).
- AGRESTI A. (1990). Categorical Data Analysis, John Wiley and Sons, New York, USA.
- AZIMI A.H., N. RAJARATNAM N. (2009). Discharge characteristics of weirs of finite crest length, journal of hydraulic engineering, vol. 135, pp. 1081-1085.
- BIJANKHAN M., DI STEFANO C.D., FERRO V., KOUCHAKZDEH S. 2014). New Stage-Discharge Relationship for Weirs of Finite Crest Length, Technical Notes, Journal of Irrigation and Drainage Engineering, Vol. 140, Issue 3.
- BOLSHAKOV V.A. (1984). Handbook of hydraulics, Kyiv, Vishcha school, 343p. (In Russian)
- BOS M.G. (1976). Discharge Measurement Structures, Laboratorium Voor Hydraulica Aan Afvoerhydrologie, Landbouwhogeschool, Wageningen, The Netherlands.

- BOS M.G. (1989). Discharge Measurement Structures, third ed., Publication 20, Int. Institute for Land Reclamation and Improvement, Wageningen, The Netherlands.
- CHOW V.T. (1959). Open-Channel Hydraulics, McGraw Hill, New York, USA.
- FILIPPOV Y.G., BRAKENI A. (2007). Use of weirs with sill of triangular profile for measurement of discharges of water in open streams and conduits,” in: Problems of Stable Development of Reclamation and Rational Resource Management: Proceedings International Science-Practice, Jubilee Conference (Kostyakov Session), Izd. VNIIA, Moscow, No 2, pp. 338-343 (In Russian).
- HENDERSON F.M. (1966). Open Channel Flow, the McMillan Company, New York, N.Y, USA.
- KHAFAGI A. (1942). Der Venturikanal: Theorie und Anwendung. Versuchsanstalt für Wasserbau, Eidgenössische Technische Hochschule Zürich, Mitteilung 1. Leemann, Zürich, Switzerland, The venturi channel: theory and application. Laboratory for Hydraulic Engineering, Swiss Federal Institute of Technology in Zurich, Communication 1, (in German).
- LANGHAAR H.L. (1951). Dimensional Analysis and Theory of Models, John Wiley and Son Ltd, 1st Edition, 166p.
- RAO N.S.G., MURALIDHAR D. (1963). Discharge characteristics of weirs of limit crest width, La Houille Blanche, No 18, pp. 537-545.
- RF STATE STANDARD MI 2406–97. (1997). Discharge of Liquid in Gravity-flow Conduits of Water-Supply and Sewer Systems, A Technique of Carrying out Measurements by Means of Standard Weirs and Flumes, Izd. GNTs NIIVODGEO and AO IRVIS, Moscow, (In Russian).
- SIA (1936). Contribution to the study of gauging methods, Bulletin 18, Schw. Wasserforschung, Bern, Switzerland, (In French).
- SPIEGEL M.R. (1974). Mathematical Handbook of Formulas and Tables, 20th Edition, McGraw Hill Inc, New York, USA.
- VOGT W.P., Johnson R.B. (2015). Dictionary of Statistics & methodology: A Nontechnical Guide for the Social Sciences, 5th Edition, SAGE Publishing.
- ZUIKOV A.L. (2017). Hydraulics of the classical Crump weir water gauge, Power Technology and Engineering, Vol. 50, Issue 6, pp. 50-59.